JOC Article

Synthesis and Spin-Trapping Properties of a New Spirolactonyl Nitrone

Yongbin Han,[†,‡] Beatrice Tuccio,[§] Robert Lauricella,[§] Antal Rockenbauer,[||] Jay L. Zweier,[‡] and Frederick A. Villamena*[,†,‡]

Department of Pharmacology and Center for Biomedical EPR Spectroscopy and Imaging, The Davis Heart and Lung Research Institute, and the Division of Cardiovascular Medicine, Department of Internal Medicine, College of Medicine, The Ohio State University, Columbus, Ohio 43210, Laboratory Chimie Provence-UMR 6264, University of Provence-CNRS, Faculty of Sciences, Saint Jerome 13397 Marseille Cedex 20, France, and Chemical Research Center, Institute of Structural Chemistry, H-1025 Budapest, Pusztaszeri 59, Hungary

frederick.villamena@osumc.edu

Received November 13, 2007

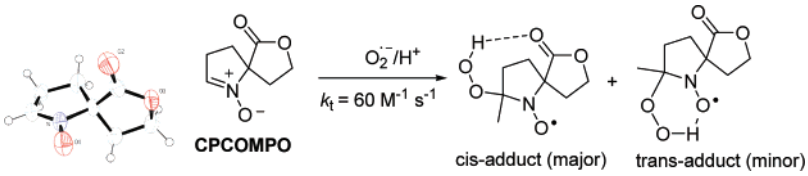

Spin trapping using electron paramagnetic resonance (EPR) spectroscopy is commonly employed for the identification of transient radicals in chemical and biological systems. A spirolactonyl-nitrone with rigid H-bond acceptor, 7-oxa-1-azaspiro[4.4]non-1-en-6-one 1-oxide, CPCOMPO, has been synthesized and characterized, and its spin-trapping properties were investigated. The rate of formation of CPCOMPO−O_2H was determined using competition kinetics between the superoxide/hydroperoxyl radical ($O_2^{\bullet-}$/$HO_2^{\bullet}$) trapping by CPCOMPO and the spontaneous dismutation of this radical in aqueous media. The rate constant of 60 $M^{-1}\cdot s^{-1}$ is the highest rate constant thus far observed at neutral pH for any nitrones using the kinetic method employed. Decay kinetics were also experimentally investigated for CPCOMPO−O_2H. The effect of rigid H-bond acceptor on the stability of the CPCOMPO−O_2H were computationally rationalized and compared to that of EMPO−O_2H, which has flexible H-bond acceptor, and results show the need of a "loose" H-bond acceptor for improved adduct stability.

Introduction

Free radicals play an important role in the initiation of oxidative damage to key biomolecular components of the cell.[1] Free radicals in unregulated concentrations have been central mediators in the pathogenesis of various diseases, such as ischemia-reperfusion injury,[2] inflammation,[3] cancer,[4] and cardiovascular diseases[5] to name a few. The one electron reduction of O_2 to superoxide radical anion ($O_2^{\bullet-}$) can lead to the production of some of the most highly oxidizing species known to be generated in biological system such as hydroxyl ($HO^{\bullet}$), peroxynitrite ($ONOO^-$), and oxidized gluthatione radical anion ($GSSG^{\bullet-}$).[1]

Spin trapping is described by the addition of short-lived free radicals to a nitrone spin trap which then gives a paramagnetic spin adduct with longer half-life that is detectable by electron paramagnetic resonance (EPR) spectroscopy (Scheme 1).[6] The pyrroline-based nitrones have been the reagent of choice for spin-trapping applications due to their ability to give finger-printable EPR spectrum upon addition to most radicals. Among the commonly used cyclic spin traps are 5,5-dimethyl-1-pyrroline *N*-oxide (DMPO), 5-diethoxyphosphoryl-5-methyl-1-

* To whom correspondence should be addressed. Tel: 614-292-8215. Fax: 614-688-0999.
† Department of Pharmacology, The Ohio State University.
‡ Center for Biomedical EPR Spectroscopy and Imaging, The Ohio State University.
§ Laboratory Chimie Provence-UMR 6264, University of Provence-CNRS.
|| Chemical Research Center, Institute of Structural Chemistry.

(1) Halliwell, B.; Gutteridge, J. M. C. *Free Radicals in Biology and Medicine*; Oxford University Press: New York, 1999.
(2) Zweier, J. L.; Talukder, M. A. H. *Cardiovasc. Res.* **2006**, *70*, 181.
(3) Petrone, W. F.; English, D. K.; Wong, K.; McCord, J. M. *Proc. Natl. Acad. Sci. U.S.A.* **1980**, *77*, 1159.
(4) Dreher, D.; Junod, A. F. *Eur. J. Cancer* **1996**, *32A*, 30.
(5) Gutierrez, J.; Ballinger, S. W.; Darley-Usmar, V. M.; Landar, A. *Circ. Res.* **2006**, *99*, 924.
(6) Villamena, F. A.; Zweier, J. L. *Antioxid. Redox Signaling* **2004**, *6*, 619.

10.1021/jo702434u CCC: $40.75
Published on Web 03/11/2008

SCHEME 1. Spin-trapping by Cyclic Nitrones

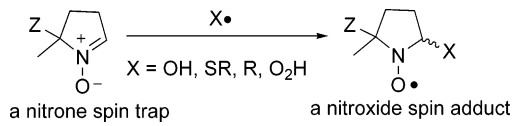

pyrroline *N*-oxide (DEPMPO), and 5-ethoxycarbonyl-5-methyl-1-pyrroline *N*-oxide (EMPO), which have shown numerous applications in the fields of fuel cell technology,[7,8] nanomaterials,[9,10] photodynamic therapy,[11] and environmental remediation[12] and in the investigation of simple organic transformations.[13] Superoxide radical anion has also been detected using spin trapping from melanosomes,[14] mitochondria,[15−18] photosynthetic systems,[19−21] nitric oxide synthase (NOS),[22−24] endothelial cells,[25,26] human neutrophils,[27,28] and reperfused heart tissue.[29−32] Nitrones have been employed as therapeutic agents in the treatment of acute stroke and ischemia-reperfusion injuries.[33,34] In in vivo systems, PBN and DMPO exhibit therapeutic properties in stroke models,[35] improvement in cerebral blood flow,[36] and NO-releasing properties.[37]

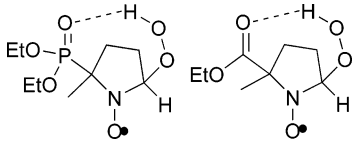

FIGURE 1. Possible stabilization of superoxide adduct of DEPMPO and EMPO using "loose" H-bond acceptors.

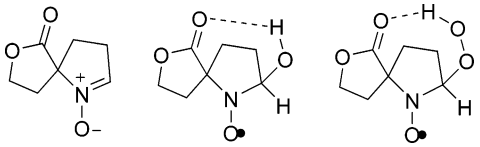

FIGURE 2. Possible stabilization of $O_2^{\bullet-}$ and $HO^{\bullet}$ adducts of CPCOMPO with a rigid hydrogen bond acceptor.

Although DMPO is the most popular spin trap for $O_2^{\bullet-}$ detection, it is still confronted by certain limitations such as poor $O_2^{\bullet-}$ trapping ability and the relatively short half-life of the $O_2^{\bullet-}$ adduct formed, thus making its formation impossible to detect in in vivo systems.[38] There is, therefore, a need to undertstand factors that governed spin trap reactivity to $O_2^{\bullet-}$ and the stability of its $O_2^{\bullet-}$ adduct. Theoretical and experimental studies showed that the presence of an electron-withdrawing substituent (such as the phosphoryl and alkoxycarbonyl moieties) in the C-5 position of the pyrroline ring increases the reactivity of nitrones to various radical species compared to the unsubstituted nitrone, DMPO.[39,40] Moreover, the presence of intramolecular H-bonding in $O_2^{\bullet-}$ (Figure 1) or $HO^{\bullet}$ adducts of phosphoryl and alkoxycarbonyl substituted nitrones has a profound effect on the stability of the spin adduct.[41,42]

Among the newly conceptualized nitrone that we have previously theoretically investigated is 6,7-oxa-1-azaspiro[4.4]-non-1-en-6-one 1-oxide (CPCOMPO), which may show a promising spin-trapping property due to its predicted high rate constant for $O_2^{\bullet-}$ trapping (Figure 2).[39,40] We have previously[39] predicted that CPCOMPO exhibited high positive charge density on the nitronyl-C, and the CPCOMPO−OH shows intramolecular −C═O---H−O− H-bond interaction with an electronic property similar to that of DEPMPO-OH. The CPCOMPO−O_2H also shows strong intramolecular H-bond interaction between C═O or N−O moieties and the hydroperoxyl-H with predicted H-bond distances of 1.9−2.0 Å indicating a possible stabilization of the $O_2^{\bullet-}$ adduct.[41] This work will investigate if cyclic nitrone with rigid spirolactonyl hydrogen-bond acceptor

(7) Bosnjakovic, A.; Schlick, S. *J. Phys. Chem. B* **2006**, *110*, 10720.
(8) Panchenko, A.; Dilger, H.; Kerres, J.; Hein, M.; Ullrich, A.; Kaz, T.; Roduner, E. *Phys. Chem. Chem. Phys.* **2004**, *6*, 2891.
(9) Yang, J.; Chen, C.; Ji H.; Ma, W.; Zhao, J. *J. Phys. Chem. B* **2005**, *109*, 21900.
(10) Yu, J.; Chen, J.; Li, C.; Wang, X.; Zhang, B.; Ding, H. *J. Phys. Chem. B* **2004**, *108*, 2781.
(11) Vakrat-Haglili, Y.; Weiner, L.; Brumfeld, V.; Brandis, A.; Salomon, Y.; McLlroy, B.; Wilson, B. C.; Pawlak, A.; Rozanowska, M.; Sarna, T.; Scherz, A. *J. Am. Chem. Soc.* **2005**, *127*, 6487.
(12) Nam, S.-N.; Han, S.-K.; Kang, J.-W.; Choi, H. *Ultrason. Sonochem.* **2003**, *10*, 139.
(13) Balakirev, M. Y.; Khramtsov, V. V. *J. Org. Chem.* **1996**, *61*, 7263.
(14) Zareba, M.; Szewczyk, G.; Sarna, T.; Hong, L.; Simon, J. D.; Henry, M. M.; Burke, J. M. *Photochem. Photobiol.* **2006**, *82*, 1024.
(15) Chen, Y.-R.; Chen, C.-L.; Yeh, A.; Liu, X.; Zweier, J. L. *J. Biol. Chem.* **2006**, *281*, 13159.
(16) Dugan, L. L.; Sensi, S. L.; Canzoniero, L. M. T.; Handran, S. D.; Rothman, S. M.; Lin, T. S.; Goldberg, M. P.; Choi, D. W. *J. Neurosci.* **1995**, *15*, 6377.
(17) Partridge, R. S.; Monroe, S. M.; Parks, J. K.; Johnson, K.; Parker, W. D., Jr.; Eaton, G. R.; Eaton, S. S. *Arch. Biochem. Biophys.* **1994**, *310*, 210.
(18) Nohl, H.; Jordan, W.; Hegner, D. *FEBS Lett.* **1981**, *123*, 241.
(19) Liu, K.; Sun, J.; Song, Y.-g.; Liu, B.; Xu, Y.-k.; Zhang, S.-x.; Tian, Q.; Liu, Y. *Photosynth. Res.* **2004**, *81*, 41.
(20) Pospisil, P.; Arato, A.; Krieger-Liszkay, A.; Rutherford, A. W. *Biochemistry* **2004**, *43*, 6783.
(21) Rahimipour, S.; Palivan, C.; Barbosa, F.; Bilkis, I.; Koch, Y.; Weiner, L.; Fridkin, M.; Mazur, Y.; Gescheidt, G. *J. Am. Chem. Soc.* **2003**, *125*, 1376.
(22) Xia, Y.; Dawson, V. L.; Dawson, T. M.; Synder, S. H.; Zweier, J. L. *Proc. Natl. Acad. Sci. U.S.A.* **1996**, *93*, 6770.
(23) Xia, Y.; Roman, L. J.; Masters, B. S. S.; Zweier, J. L. *J. Biol. Chem.* **1998**, *273*, 22635.
(24) Xia, Y.; Tsai, A.-L.; Berka, V.; Zweier, J. L. *J. Biol. Chem.* **1998**, *273*, 25804.
(25) Serrano, C. V., Jr.; Mikhail, E. A.; Wang, P.; Noble, B.; Kuppusamy, P.; Zweier, J. L. *Biochim. Biophys. Acta* **1996**, *1316*, 191.
(26) Varadharaj, S.; Watkins, T.; Cardounel, A. J.; Garcia, J. G. N.; Zweier, J. L.; Kuppusamy, P.; Natarajan, V.; Parinandi, N. L. *Antioxid. Redox Signaling* **2005**, *7*, 287.
(27) Jackson, H. L.; Cardounel, A. J.; Zweier, J. L.; Lockwood, S. F. *Bioorg. Med. Chem. Lett.* **2004**, *14*, 3985.
(28) Sankarapandi, S.; Zweier, J. L.; Mukherjee, G.; Quinn, M. T.; Huso, D. L. *Arch. Biochem. Biophys.* **1998**, *353*, 312.
(29) Wang, P.; Chen, H.; Qin, H.; Sankarapandi, S.; Becher, M. W.; Wong, P. C.; Zweier, J. L. *Proc. Natl. Acad. Sci. U.S.A.* **1998**, *95*, 4556.
(30) Zweier, J. L.; Flaherty, J. T.; Weisfeldt, M. L. *Proc. Natl. Acad. Sci. U.S.A.* **1987**, *84*, 1404.
(31) Zweier, J. L.; Kuppusamy, P.; Lutty, G. A. *Proc. Natl. Acad. Sci. U.S.A.* **1988**, *85*, 4046.
(32) Zweier, J. L.; Kuppusamy, P.; Williams, R.; Rayburn, B. K.; Smith, D.; Weisfeldt, M. L.; Flaherty, J. T. *J. Biol. Chem.* **1989**, *264*, 18890.
(33) Konorev, E. A.; Baker, J. E.; Joseph, J.; Kalyanaraman, B. *Free Radical Biol. Med.* **1993**, *14*, 127.
(34) Zhao, Z.; Cheng, M.; Maples, K. R.; Ma, J. Y.; Buchan, A. M. *Brain Res.* **2001**, *909*, 46.
(35) Saito, K.; Cutler, R. G. *Oxid. Stress Aging* **1995**, 379.
(36) Inanami, O.; Kuwabara, M. *Free Radical Res.* **1995**, *23*, 33.
(37) Locigno, E. J.; Zweier, J. L.; Villamena, F. A. *Org. Biomol. Chem.* **2005**, *3*, 3220.
(38) Khan, N.; Wilmot, C. M.; Rosen, G. M.; Demidenko, E.; Sun, J.; Joseph, J.; O'Hara, J.; Kalyanaraman, B.; Swartz, H. M. *Free Radical Biol. Med.* **2003**, *34*, 1473.
(39) Villamena, F. A.; Hadad, C. M.; Zweier, J. L. *J. Am. Chem. Soc.* **2004**, *126*, 1816.
(40) Villamena, F. A.; Xia, S.; Merle, J. K.; Lauricella, R.; Tuccio, B.; Hadad, C. M.; Zweier, J. L. *J. Am. Chem. Soc.* **2007**, *129*, 8177.
(41) Villamena, F. A.; Hadad, C. M.; Zweier, J. L. *J. Phys. Chem. A* **2005**, *109*, 1662.
(42) Villamena, F. A.; Rockenbauer, A.; Gallucci, J.; Velayutham, M.; Hadad, C. M.; Zweier, J. L. *J. Org. Chem.* **2004**, *69*, 7994.

SCHEME 2. Synthesis of CPCOMPO

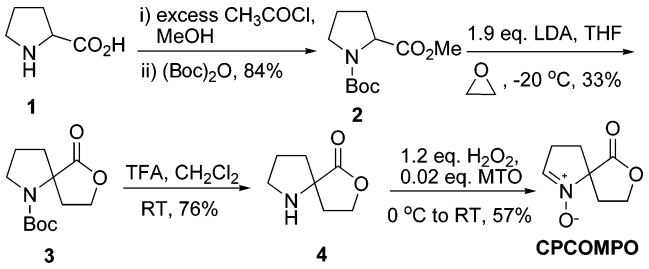

at C-5 position could considerably enhance (or worsen) the $O_2^{\bullet-}$ and $HO^{\bullet}$ adducts' stability compared to those with "loose" H-bond acceptors found in EMPO and DEPMPO.

Results and Discussion

Synthesis and Characterization. The preparation of CPCOMPO is shown in Scheme 2 demonstrating a new methodology for the synthesis of cyclic nitrones without employing the usual reductive cyclization of nitro aldehydes. Boc-deprotection of **3** was achieved in CH_2Cl_2 using TFA to afford compound **4**. The oxidation of secondary amine to nitrone using the conventional reagents such as $Na_2WO_4-H_2O_2$,[21] *m*-CPBA,[22] and $HOAc-H_2O_2$[23] were inefficient. The use of methyltrioxorhenium(VII) (MTO)$-H_2O_2$,[43−45] however, oxidized **4** to nitrones and gave a relatively high yield (see the Experimental Section). Spectroscopic data are consistent with the presence of nitrone moiety with ^{1}H NMR peaks at 7.0 ppm and IR peaks at 1583 cm^{-1} and 1226 cm^{-1} for C═N and N−O, respectively.[46] The structure of CPCOMPO was also confirmed by X-ray crystallography with a racemic space group of $P2_1/c$ (Figure 3).

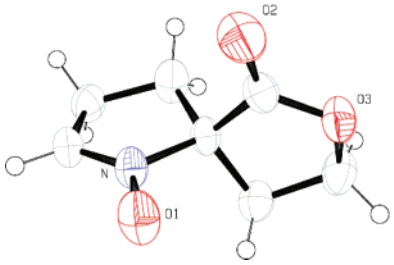

FIGURE 3. ORTEP figure for CPCOMPO.

Spin Trapping Studies. (a) Superoxide Radical Anion. In this study, superoxide, $O_2^{\bullet-}$, and its protonated form, $HO_2^{\bullet}$, were not distinguished since both radicals lead to the same EPR-detectable spin adduct CPCOMPO$-O_2H$ in aqueous media. With the aim of simplifying the notation, the term "superoxide" will be used to designate both superoxide and hydroperoxyl radicals as a whole. Similarly, the symbol "$O_2^{\bullet-}$" will represent either protonated or nonprotonated forms of the radical. Figure 4 shows the EPR spectra of CPCOMPO$-O_2H$, the $O_2^{\bullet-}/HO_2^{\bullet}$ adduct, generated from various radical sources and gave a common spectral profile. For simplicity, computer simulation of the spectra only assumed the presence of two species. The

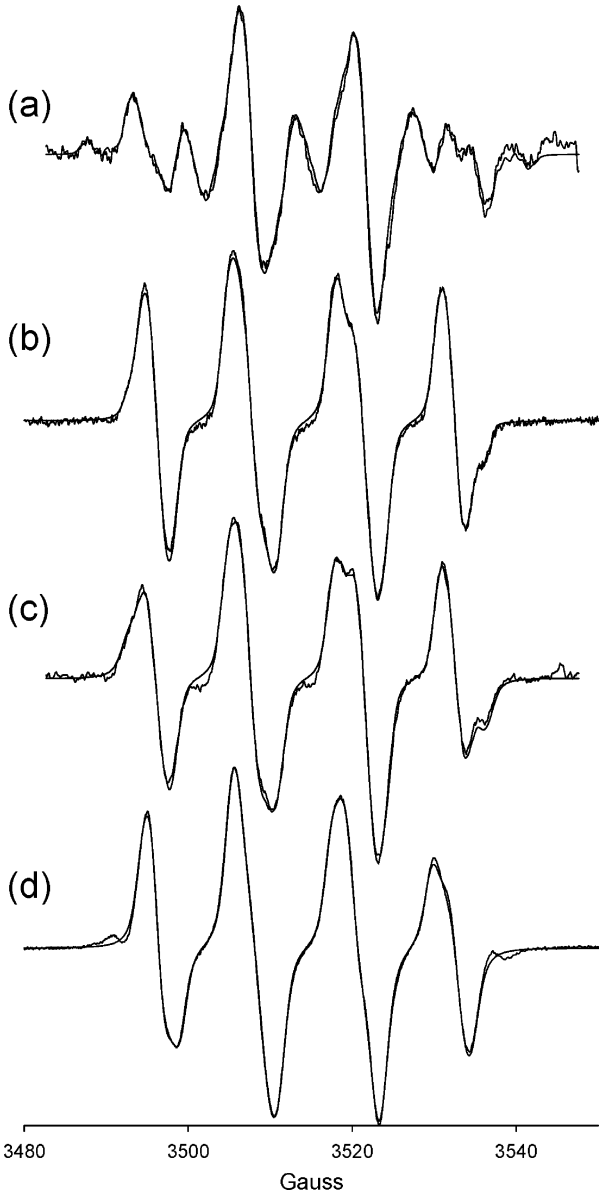

FIGURE 4. X-band EPR spectra of CPCOMPO$-O_2H$ generated from (a) light- riboflavin (36%): a_N = 12.6 G, $a_{\beta-H}$ =10.3 G; $HO^{\bullet}$ adduct (38%); alkyl adduct (9%): a_N = 13.8 G, $a_{\beta-H}$ = 22.1 G; unknown triplet product (17%): a_N = 14.2 G; (b) KO_2 in DMSO, I (81%): a_N = 12.9 G, $a_{\beta-H}$ =10.3 G, $a_{\gamma-H}$ = 1.4 G; II (11%): a_N = 13.2 G, $a_{\beta-H}$ = 11.1 G, $a_{\gamma-H}$ = 1.0 G; $HO^{\bullet}$ adduct (7%); (c) xanthine−xanthine oxidase, I (62%): a_N = 13.0 G, $a_{\beta-H}$ =10.0 G, $a_{\gamma-H}$ = 1.5 G; II (17%): a_N = 13.1 G, $a_{\beta-H}$ = 11.5 G, $a_{\gamma-H}$ = 1.1 G; $HO^{\bullet}$ adduct (20%); (d) H_2O_2 in pyridine, I (43%), a_N = 13.2 G, $a_{\beta-H}$ = 11.2 G, $a_{\gamma-H}$ = 0.9 G; II (57%), a_N = 12.3 G, $a_{\beta-H}$ = 9.6 G, $a_{\gamma-H}$ = 1.6 G. Simulated spectra are shown as trace plots.

spectra reveal the presence of $O_2^{\bullet-}$ adduct and significant contamination from the $HO^{\bullet}$ adduct (the $HO^{\bullet}$ adduct can be formed from the decomposition of the $O_2^{\bullet-}$ adduct). Computational studies show that the formation of *cis*-CPCOMPO$-O_2^-$ is more energetically preferred by 3.1 kcal/mol over the trans adduct at the PCM/B3LYP/6-31+G**//B3LYP/6-31G* level (Table 1). Our previous studies[47−49] showed that at neutral pH the initial addition of $O_2^{\bullet-}$ to nitrones occurs followed by

(43) Saladino, R.; Neri, V.; Cardona, F.; Goti, A. *Adv. Synth. Catal.* **2004**, *346*, 639.
(44) Goti, A.; Nannelli, L. *Tetrahedron Lett.* **1996**, *37*, 6025.
(45) Murray, R. W.; Iyanar, K.; Chen, J.; Wearing, J. T. *J. Org. Chem.* **1996**, *61*, 8099.
(46) Breuer, E.; Aurich, H. G.; Nielsen, A. *Nitrones, Nitronates, and Nitroxides*; John Wiley & Sons: New York, 1989.
(47) Villamena, F. A.; Hadad, C. M.; Zweier, J. L. *J. Phys. Chem. A* ***2005***, *109*, *1662*.
(48) Villamena, F. A.; Merle, J. K.; Hadad, C. M.; Zweier, J. L. *J. Phys. Chem. A* **2005**, *109*, 6083.

TABLE 1. Free Energies of Reaction (in kcal/mol) of CPCOMPO with Various Radicals at the PCM/B3LYP/6-31+G//B3LYP/6-31G* Level at 298 K**

adducts	$\Delta G_{rxn,aq}$	adducts	$\Delta G_{rxn,aq}$
$HO_2^\bullet$		$O_2^{\bullet-}$	
cis	−5.2	cis	9.2
trans	−4.9	trans	12.3
$HO^\bullet$		$SO_3^{\bullet-}$ (S-centered)	
cis	−35.4	cis	1.8
trans	−38.6	trans	3.0
$CH_3^\bullet CHOH$		$SO_3^{\bullet-}$ (O-centered)	
cis	−16.2	cis	5.9
trans	−19.1	trans	3.8
t−$BuO^\bullet$		$MeS^\bullet$	
cis	−12.8	cis	−6.7
trans	−17.9	trans	−6.4
$CO_2^{\bullet-}$			
cis	−12.9		
trans	−13.8		

SCHEME 3. Mechanism of the Formation of CPCOMPO−O_2H in Neutral pH

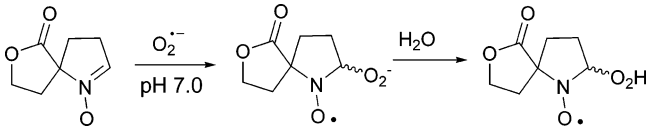

proton abstraction from water by the hydroperoxide to form the final adduct nitrone−O_2H as evidenced by the endoergic free energies and low bimolecular rate constant of this reaction at pH 7.0.[50] It can, therefore, be assumed that the major diastereoisomer of CPCOMPO−O_2H formed in solution is the cis isomer as determined by the preference of *cis*-CPCOMPO−O_2^- formation over the trans isomer prior to protonation (see Scheme 3).

The calculated hyperfine splitting constants (hfsc) (a_x) at the PCM/B3LYP/6-31+G**//B3LYP/6-31G* for the respective *cis*- and *trans*-CPCOMPO−O_2H, and by only considering the bulk dielectric effect of water solvent, gave lower hfsc's for the cis isomer, i.e., $a_N = 10.5$ G and $a_{\beta-H} = 6.8$ G, compared to the trans adduct with $a_N = 11.7$ G and $a_{\beta-H} = 8.2$ G. An extensive computational study on the prediction of hfsc's of DMPO−OOH and DMPO−OH adducts was previously reported[51] and showed that the overall effect of the level of theory on the Boltzmann-weighted hfsc's for DMPO−OOH conformations is negligible whether at the B3LYP/6-31+G**//B3LYP/6-31G* or CBS-QB3. Furthermore, it has been demonstrated by Saracino et al.[52] that the presence of two explicit water molecules interaction with nitroxides bearing no β-hydrogen (CP and CT), and with consideration of the bulk dielectric effect of water, gave significant improvement in the calculated a_N value compared to in the absence of water interaction.

Similarly, we showed[51] improvement in the Boltzmann-average values of the calculated a_N of the various conformers of DMPO−OOH relative to the experimental a_N using model that includes two explicit water molecules and bulk dielectric

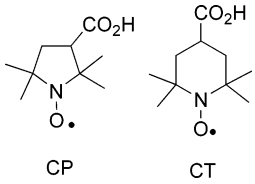

CP CT

effect of water at the PCM/B3LYP/6-31+G**//B3LYP/6-31G*. However, prediction of the $a_{\beta-H}$ was overestimated by about 1.9 G. In order to improve the predicted a_N and $a_{\beta-H}$ values for CPCOMPO−O_2H values, a model that includes explicit water molecule interaction was employed at the same level of theory. The Boltzmann-averaged a_N and $a_{\beta-H}$ values for the two conformations of cis CPCOMPO−O_2H·$(H_2O)_2$ were 7.5 and 3.4 G, respectively, while $a_N = 12.0$ G and $a_{\beta-H} = 9.3$ G were predicted for the trans adducts. Although the trends in the relative a_N and $a_{\beta-H}$ values for the cis and trans adducts for CPCOMPO−O_2H versus CPCOMPO−O_2H·$(H_2O)_2$ are similar, the latter gave less accurate values. The use of three explicit molecules followed similar trends (except for a_N) in the relative values for cis and trans isomers but accuracy is greatly compromised. On the basis of four preferred conformations for each of the cis and trans CPCOMPO−O_2H·$(H_2O)_3$ adducts, the calculated Boltzmann-averaged values for cis adducts were $a_N = 11.0$ G and $a_{\beta-H} = 2.6$ G and $a_N = 10.2$ G and $a_{\beta-H} = 8.3$ G for the trans adducts. It should be noted that the qualitative trends in the hfsc values are more relevant in this study since β-hydrogen hfsc seems to be more problematic to predict accurately. It has been noted in previous works[51,53] that factors such as dynamic effects due to the variation in the pyramidalization of the nitroxides moiety as well as sensitivity of the $a_{\beta-H}$ to the fluxional conformation of the hydroperoxyl moiety should be taken into account for the accurate prediction of hfsc's.

Figure 4 shows the experimental spectra of the CPCOMPO−O_2H from various $O_2^{\bullet-}$ generating systems. The spectrum arising from the use of light-riboflavin $O_2^{\bullet-}$ generating system (Figure 4a) gave a significant contamination amount of an unknown decomposition product with a triplet feature and a C-centered radical adduct. Superoxide adduct concentrations generated from KO_2, xanthine−xanthine oxidase, and H_2O_2−pyridine (Figure 4b−d) are significantly high (>80%) compared to the $HO^\bullet$ adduct with negligible presence of artifactual adducts as observed for the light-riboflavin system. Due to the presence of multiple species in Figure 4a, the decomposition of CPCOMPO−O_2H to its diastereomeric components by simulation was not successful. However, Figure 4b,c gave reasonably clean spectra that allow the simulation of the two diastereomeric forms of CPCOMPO−O_2H. In both cases, the major adduct formed gave lower hfsc values for nitrogen and β-H compared to the minor adduct formed. These results may suggest that the major adduct formed is the *cis*-CPCOMPO−O_2H consistent with the thermodynamic preference of $O_2^{\bullet-}$ addition to CPCOMPO at the cis position and the qualitative predicted trends in the hfsc's for the cis and trans CPCOMPO−O_2H. However, simulation of the EPR spectrum in pyridine (Figure 4d) yielded two diastereoisomeric adducts in almost equal yields in which the species with a lower $a_{\beta-H}$ of 9.6 G is still slightly more predominant (57%) than the species with higher $a_{\beta-H}$ of 11.2 G at 43%. It should be noted that by using H_2O_2−pyridine, the $O_2^{\bullet-}$ adduct is formed not through spin trapping but via

(49) Villamena, F. A.; Xia, S.; Merle, J. K.; Lauricella, R.; Tuccio, B.; Hadad, C. M.; Zweier, J. L. *J. Am. Chem. Soc.* **2007**, *129* 8177.
(50) Allouch, A.; Lauricella, R. P.; Tuccio, B. N. *Mol. Phys.* **2007**, *105*, 2017.
(51) Villamena, F. A.; Merle, J. K.; Hadad, C. M.; Zweier, J. L. *J. Phys. Chem. A* **2005**, *109*, 6089.
(52) Saracino, G. A. A.; Tedeschi, A.; D'Errico, G.; Improta, R.; Franco, L.; Ruzzi, M.; Corvaia, C.; Barone, V. *J. Phys. Chem. A* **2002**, *106*, 10700.
(53) Eriksson, L. A.; Wang, J.; Boyd, R. J.; Lunell, S. *J. Phys. Chem.* **1994**, *98*, 792.

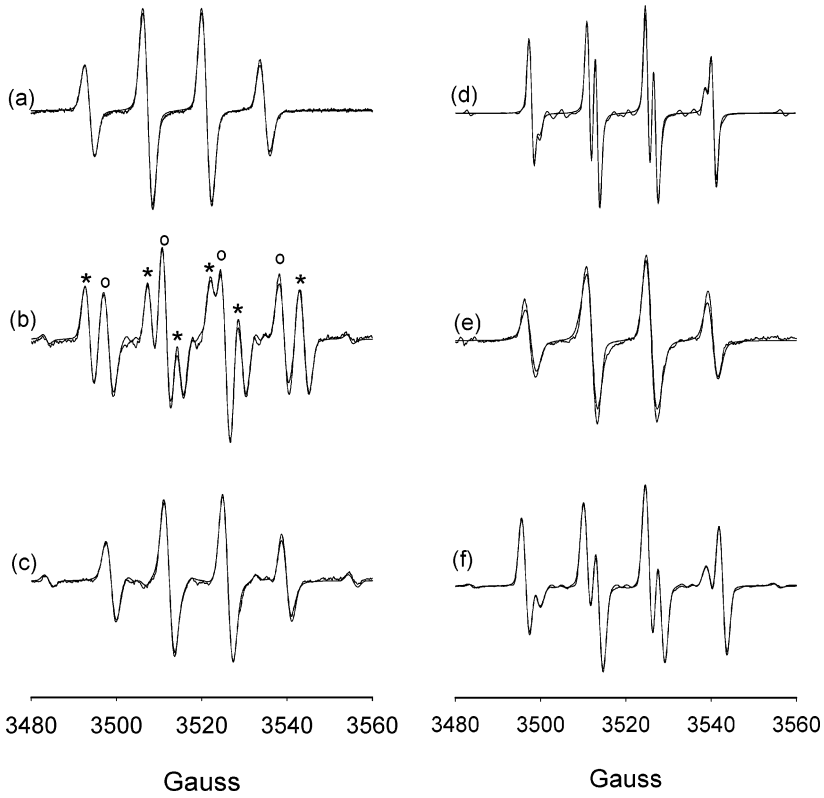

FIGURE 5. X-band EPR spectra of various radical adducts of CPCOMPO: (a) hydroxyl radical: $g = 2.00550$, $a_N = 13.9$ G, $a_{\beta-H} = 13.4$ G; (b) α-hydroxyethyl radical (marked by *) (43%): $g = 2.00528$, $a_N = 14.7$ G, $a_{\beta-H} = 21.0$ G; OR radical (marked by o) (42%): $g = 2.00539$, $a_N = 14.0$ G, $a_{\beta-H} = 13.3$ G; (c) *tert*-butoxy radical: $g = 2.00541$, $a_N = 14.0$ G, $a_{\beta-H} = 13.2$ G; (d) sulfite radical, I (79%): $g = 2.00530$, $a_N = 13.7$ G, $a_{\beta-H} = 15.4$ G; II (21%): $g = 2.00532$, $a_N = 13.9$ G, $a_{\beta-H} = 12.1$ G); (e) glutathionyl radical: $g = 2.00561$, $a_N = 14.6$ G, $a_{\beta-H} = 13.4$ G; (f) carbon dioxide radical anion: $g = 2.00523$, $a_N = 14.5$ G, $a_{\beta-H} = 17.3$ G. Simulated spectra are shown as trace plots.

nucleophilic addition of the HOO^- and subsequent oxidation of the resulting hydroxylamine to nitroxide as previously proposed.[54,55]

(b) Hydroxyl and Other Radicals. The EPR spectrum of CPCOMPO−OH generated from the Fenton reaction is shown in Figure 5a. Unlike the $HO^•$ adduct of EMPO and BMPO (or BocMPO),[56] the hfsc's for the cis and trans products for CPCOMPO are difficult to discern. Figure 5b−f shows the EPR spectra for the α-hydroxyethyl ($CH_2^•CHOH$), *tert*-butoxy (*t*-$BuO^•$), sulfite ($SO_3^{•-}$), glutathione ($GS^•$), and carbon dioxide anion ($CO_2^{•-}$) radical adducts of CPCOMPO, each with distinctive hfsc parameters.

The calculated free energies of reaction at the PCM/B3LYP/6-31+G**// B3LYP/6-31G* level for the formation of the various adducts are shown in Table 1. Unlike in the formation of $HO_2^•$ and $O_2^{•-}$ adduct in which the cis isomers are possibly preferred, the formation of trans isomers are more favored for the $HO^•$, $CH_3^•CHOH$, *t*-$BuO^•$, and $CO_2^{•-}$ adducts (relative Boltzmann ratios of the cis and trans adduct are shown in the Supporting Information). The thermodynamics of $GS^•$ addition can be represented by the addition of $MeS^•$ for simplicity and gave almost the same exoergic free energies of ∼−6.5 kcal/mol for the cis and trans adduct formation.

The $SO_3^{•-}$ adduct gave a high proportion of the cis and trans forms as shown in Figure 5d with identical *g* factors and almost similar a_N values. The observed hfsc values for the CPCOMPO−SO_3 was close to those observed in the $SO_3^{•-}$ adducts of EMPO[57] and DMPO.[58] Computational studies show that although the formation of CPCOMPO−SO_3 is endoergic, the free energy difference for the formation of S- and O-centered adducts is only about 0.8 kcal/mol according to Table 1, with the cis and trans isomers being favored for the S- and O-centered adducts, respectively. Due to the similarities in the energetics of S- and O-centered CPCOMPO−SO_3 formation, it can be assumed that both products are formed in solution as shown in Figure 6. Natural population analysis (NPA) of the charge densities for the trigonal pyramidal, $SO_3^{•-}$, gave a −0.98 e charge on each of the 3 O atoms and a +1.94 e positive charge on the S atom. Spin density distribution is 19% and 43% on each of the O and S atoms, respectively. The high spin density distribution on the O and S atoms of $SO_3^{•-}$ could explain the favorability of formation of both O- and S-centered CPCOMPO−SO_3. The dependence of the mode of radical addition to nitrones on the spin density distribution of the radical had been discussed in our previous works.[59]

Kinetics and Computational Studies. (a) Rate of Formation of CPCOMPO−O_2H Adduct. The kinetic method used in the present work, based on a competition between the superoxide trapping and its spontaneous dismutation at pH 7, has been extensively described elsewhere and was employed

(54) Barbati, S.; Clement, J. L.; Olive, G.; Roubaud, V.; Tuccio, B.; Tordo, P. ^{13}P labeled cyclic nitrones: A new class of spin traps for free radicals in biological milieu. In *Free Radicals in Biology, Environment*; Minisci, F., Ed.; Kluwer Academic Publishers: Dordrecht, The Netherlands, 1997; p 39.

(55) Tuccio, B.; Zeghdaoui, A.; Finet, J.-P.; Cerri, V.; Tordo, P. *Res. Chem. Intermed.* **1996**, *22*, 393.

(56) Villamena, F. A.; Hadad, C. M.; Zweier, J. L. *J. Phys. Chem. A* **2003**, *107*, 4407.

(57) Olive, G.; Mercier, A.; Le Moigne, F.; Rockenbauer, A.; Tordo, P. *Free Radical Biol. Med.* **2000**, *28*, 403.

(58) Potapenko, D. I.; Bagryanskaya, E. G.; Reznikov, V. V.; Clanton, T. L.; Khramtsov, V. V. *Magn. Reson. Chem.* **2003**, *41*, 603.

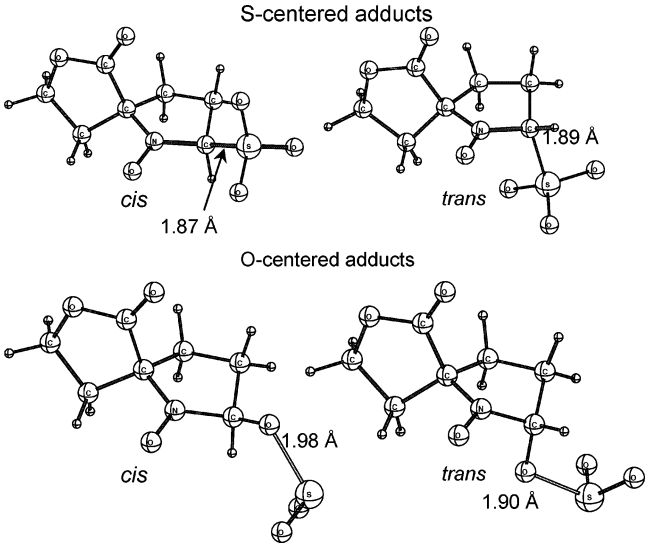

FIGURE 6. Sulfite radical anion adducts of CPCOMPO. See Table 1 for the respective free energies of reaction.

SCHEME 4. Reactions 1−4 Considered in the Kinetic Model

$$X/XO \xrightarrow{O_2,\ k_x} O_2^{\bullet-} \quad (1)$$

$$2\,O_2^{\bullet-} + 2\,H^+ \xrightarrow{k_{dis}} O_2 + H_2O_2 \quad (2)$$

$$O_2^{\bullet-} + CPCOMPO + H^+ \xrightarrow{k_t} CPCOMPO\text{-}O_2H \quad (3)$$

$$CPCOMPO\text{-}O_2H \xrightarrow{k_d} Y \quad (4)$$

SCHEME 5. Rate Equations 5−8 Considered in the Kinetic Model

$$d[X]/dt = -k_x[X] \quad (5)$$

$$d[O_2^{\bullet-}]/dt = k_x[X] - k_t[CPCOMPO][O_2^{\bullet-}] - 2k_{dis}[O_2^{\bullet-}]^2 \quad (6)$$

$$d[CPCOMPO\text{-}O_2H]/dt = k_t[CPCOMPO][O_2^{\bullet-}] - k_d[CPCOMPO\text{-}O_2H] \quad (7)$$

$$d[CPCOMPO]/dt = -k_t[CPCOMPO][O_2^{\bullet-}] \quad (8)$$

for several linear and cyclic nitrones.[40,60−62] The method does not require calibration of the initial superoxide concentration. EPR spectra of CPCOMPO−O_2H were recorded as a function of time at various CPCOMPO concentrations, and kinetic curves were obtained after treatment of these spectra using both singular value decomposition (SVD) and pseudo-inverse deconvolution methods. Modeling these curves allowed the determination of the rate constants k_t and k_d for the superoxide trapping and the adduct decay reactions, respectively.

The kinetic model used can be described by reactions 1−4 (Scheme 4), in which k_{dis}, k_d, and k_t are the rate constants for the superoxide spontaneous dismutation, for the pseudo-first-order decay of CPCOMPO−O_2H, and for the spin trapping of superoxide, respectively, and Y represents the EPR-silent products. The apparent rate constant for the trapping reaction by the nitrones, k_t, has been demonstrated[50] to be pH dependent and includes the contribution of both $HO_2^{\bullet}$ and $O_2^{\bullet-}$ trapping. At pH 7, k_{dis} is equal to 635×10^3 $M^{-1}\cdot s^{-1}$,[50] and the rate eqs 5−8 given in Scheme 5 can be written on the basis of these reactions.

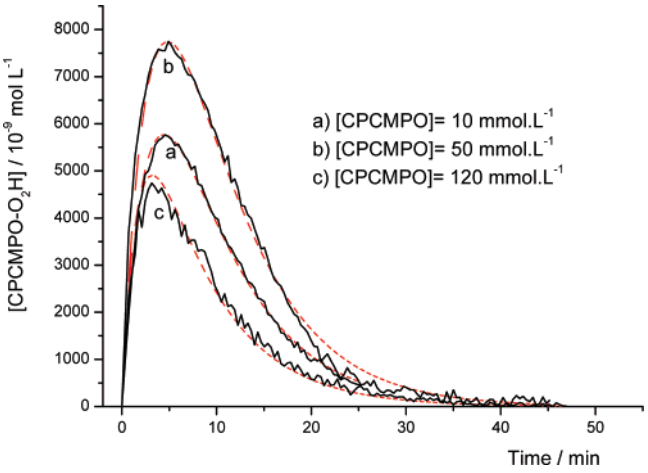

FIGURE 7. Experimental (black) and calculated (red) kinetic curves indicating the time-dependent changes in the CPCOMPO−O_2H concentration as a function of CPCOMPO concentration at pH 7.0.

TABLE 2. Rate Constants for the Spin Trapping of Superoxide by Nitrones (k_t) and for the Decay of Nitrone/Superoxide Spin Adducts (k_d) at pH 7.0

curve	[CPCOMPO]/mM	$k_d/10^{-3}$ s^{-1}	k_t/M^{-1} s^{-1}
a	10	6.1 ± 0.2	
b	50	4.8 ± 0.2	60 ± 4
c	120	9.6 ± 0.2	

Figure 7 shows the formation and decay of CPCOMPO−O_2H as a function of time after deconvolution of the experimental plots. As shown in Table 2, curve fitting of the three experimental plots yielded kinetic rate constants, k_t and k_d. The calculated rate of formation was $k_t = 60 \pm 4$ $M^{-1}\cdot s^{-1}$, which is higher compared to that observed at pH 7.2 for EMPO[60−62] and AMPO,[40] of 10.9 and 25.2 $M^{-1}\cdot s^{-1}$, respectively, using the same kinetic method as previously reported. The theoretically determined rate constant of 3.1 $M^{-1}\cdot s^{-1}$ (at the PCM/mPW1K/6-31+G** level) for the trapping of $O_2^{\bullet-}$ by CPCOMPO is intermediate in reactivity compared to other nitrones considered in our previous study.[40] Using the same experimental conditions and method of kinetic analysis, the second-order rate constant reported for other nitrones are as follows (in $M^{-1}\cdot s^{-1}$): DEPO (31.1);[60] AMPO (25.2);[40] EMPO (10.9);[62] DEPMPO (3.95);[62] BocMPO (3.45);[63] DMPO (2.0).[62] Therefore, the experimental rate constant of 60 $M^{-1}\cdot s^{-1}$ for CPCOMPO is by far the fastest experimentally observed for any nitrones.

The reactivity of the carbonyl-C to $O_2^{\bullet-}$ was also explored since, like nitrones, the carbonyl group maybe susceptible to nucleophilic attack from $O_2^{\bullet-}$. Figure 8 shows the addition reaction of $O_2^{\bullet-}$ to the carbonyl-C moiety of CPCOMPO. The free energy of $O_2^{\bullet-}$ addition to the carbonyl-C trans to the nitronyl moiety is 11.7 kcal/mol endoergic and more preferred

(59) Villamena, F. A.; Locigno, E. J.; Rockenbauer, A.; Hadad, C. M.; Zweier, J. L. *J. Phys. Chem. A* **2006**, *110*, 13253.
(60) Allouch, A.; Roubaud, V.; Lauricella, R.; Bouteiller, J.-C.; Tuccio, B. *Org. Biomol. Chem* **2005**, *3*, 2458.
(61) Lauricella, R.; Allouch, A.; Roubaud, V.; Bouteiller, J.-C.; Tuccio, B. *Org. Biomol. Chem.* **2004**, *2*, 1304.
(62) Lauricella, R. P.; Bouteiller, J.-C. H.; Tuccio, B. N. *Phys. Chem. Chem. Phys.* **2005**, *7*, 399.
(63) Allouch, A.; Roubaud, V.; Lauricella, R.; Bouteiller, J.-C.; Tuccio, B. *Org. Biomol. Chem.* **2003**, *1*, 593.

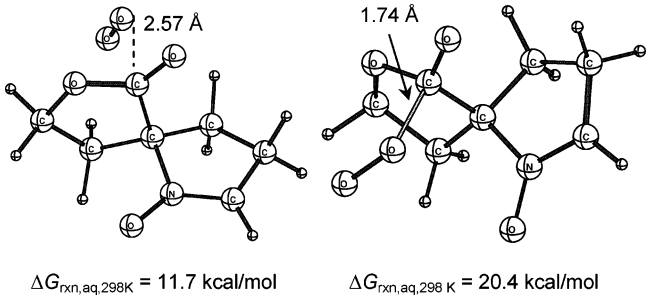

FIGURE 8. Superoxide radical cis (left) and trans (right) addition to the carbonyl-C of CPCOMPO.

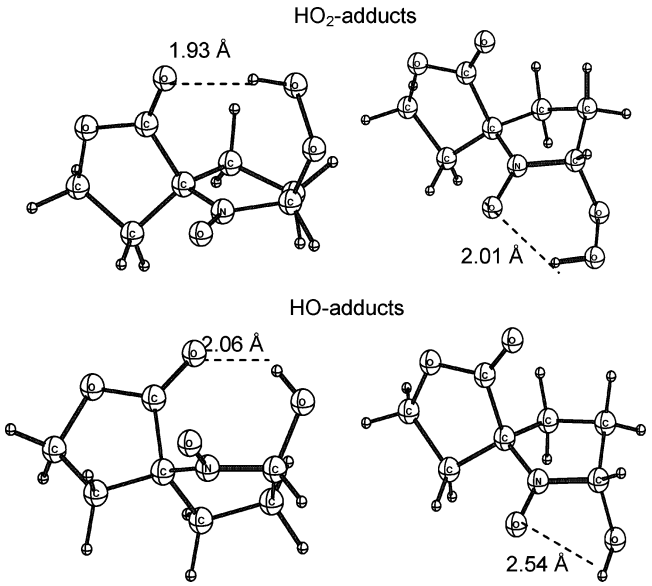

FIGURE 9. Hydroxyl and hydroperoxyl adducts of CPCOMPO showing intramolecular H-bonding interactions.

than the corresponding cis addition reaction. Considering that the calculated free energy of $O_2^{\bullet-}$ addition to the nitronyl-C is 9.2 kcal/mol (Table 1), which is about 2.5 kcal/mol more preferred than addition to carbonyl-C, it can be inferred that the most preferred reaction of $O_2^{\bullet-}$ to CPCOMPO is via addition to the nitronyl-C.

(b) Decay Rates of CPCOMPO−O_2H and CPCOMPO−OH Adducts. The half-life of CPCOMPO−O_2H was found to be only $t_{1/2} \sim 2.4$ min when the concentration of CPCOMPO was 50 mM (see Table 2). Although the decay rate of nitrone O_2H depends on many factors, such as the nitrone concentration or the $O_2^{\bullet-}$ generating system used, this value is significantly shorter compared to that of BMPO (or BocMPO)[64] and EMPO with $t_{1/2} \sim 9$ and 14 min, respectively. This kinetic result suggests that rigid H-bond acceptor has a significant effect on the HO_2-adduct stability. This instability of CPCOMPO−O_2H is probably due to the formation of a rigid 8- or 7-membered ring system (assuming that cis adduct is more favored than the trans adduct based on Table 1) that is formed upon intramolecular H-bonding of hydroperoxyl-H with carbonyl-O and nitronyl-O, respectively (see Figure 9). Unlike the EMPO and BMPO analogues, the ester moiety is "loose" and can have flexibility in maintaining the H-bonding interaction with the hydroperoxyl-H and, therefore, may be responsible for their longer half-lives. The effect of trans adduct, however, on the overall half-lives of the $O_2^{\bullet-}$ adduct should cancel out since the N−O---H−O_2 is the common H-bond interaction among the trans adducts of CPCOMPO, EMPO, and BMPO as we previously reported[47,49,65] with the N−O moiety in all of the adducts having similar conformation. The inductive effect of substituents at the C-5 position on the C−N bond breaking process, however, may also play an important role in the unimolecular decomposition of the adducts regardless of the presence of intramolecular H-bonding and is now currently being investigated in our laboratory.

The kinetics of decay of CPCOMPO−OH was also investigated using H_2O_2 photolysis. An analysis of the decay plots for CPCOMPO−OH and EMPO−OH fit pure first order for the first 17 min of decay. The calculated first-order rate constants for CPCOMPO−OH and EMPO−OH decomposition were $1.13 \pm 0.03 \times 10^{-3}$ s^{-1} and $5.66 \pm 0.29 \times 10^{-4}$ s^{-1}, respectively. The corresponding half-lives of ~ 10.2 min for CPCOMPO−OH and 20.4 min for EMPO−OH are significantly different from each other. The most preferred diastereomeric product for CPCOMPO−OH is the trans form (99% Boltzmann weighed) while equal preference for cis and trans adduct formation has been predicted for EMPO−OH,[66,67] suggesting that intramolecular C═O----HO H-bonding is not present in CPCOMPO−OH adduct and possibly plays a role in the stabilization of EMPO-OH adduct.

Conclusion

CPCOMPO was synthesized and characterized, and its spin-trapping properties were investigated and found to exhibit discernible EPR spectral profiles for various spin adducts. Computational studies using DFT show $O_2^{\bullet-}$ addition to lactonyl-O is less favored compared to addition to nitronyl-C. Using a kinetic approach for the evaluation of rate constant, CPCOMPO gave second-order rate constant for $HO_2^{\bullet}/O_2^{\bullet-}$ addition of $k_t = 60$ $M^{-1}{\cdot}s^{-1}$, which is the highest rate constant observed thus far for a nitrone using the kinetic model developed by Tuccio et al. The half-life of CPCOMPO−O_2H, however, seems to be compromised by the presence of a rigid H-bond acceptor. Therefore, strong intramolecular H-bonding in the presence of flexible H-bond acceptor should be taken into account in the design of new spin traps for longer HO_2-adduct stability. Moreover, since spirolactone moiety is found in natural products[68] and have exhibited biological activity such as antagonist of the aldosterone receptors of the epithelial cells,[69] the presence of spirolactonyl moiety along with the high $O_2^{\bullet-}$ scavenging ability of the nitronyl group in CPCOMPO can have interesting pharmacological applications.

Experimental Section

Pyrrolidine-1,2-dicarboxylic Acid 1-*tert*-Butyl Ester 2-Methyl Ester (2). Compound **2** was prepared according to the procedure described elsewhere[70] but using proline **1** (26.2 g, 228 mmol) as a

(64) Villamena, F. A.; Zweier, J. L. *J. Chem. Soc., Perkin Trans. 2* **2002**, 1340.

(65) Villamena, F. A.; Merle, J. K.; Hadad, C. M.; Zweier, J. L. *J. Phys. Chem. A.* **2007**, *111*, 9995.

(66) Villamena, F. A.; Hadad, C. M.; Zweier, J. L. *J. Phys. Chem. A* **2003**, *107*, 4407.

(67) Villamena, F. A.; Hadad, C. M.; Zweier, J. L. *J. Am. Chem. Soc.* **2004**, *126*, 1816.

(68) Ramsay, L. E.; Shelton, J. R.; Wilkinson, D.; Tidd, M. J. *Br. J. Clin. Pharm.* **1976**, *3*, 607.

(69) Doggrell, S. A.; Brown, L. *Expert Opin. Invest. Drugs* **2001**, *10*, 943.

starting material to yield 37.0 g (98%) of crude proline methyl ester hydrochloride. The crude salt (20 g, 120 mmol) was used without further purification to give compound **2** (23.8 g, 86%). ^{1}H NMR (400 MHz, $CDCl_3$, ppm): δ 1.39 and 1.43 (s, Boc rotamers 9H), 1.80−2.00 (m, 3H), 2.12−2.28 (m, 1H), 3.31−3.56 (m, 2H), 3.73 (s, 3H), 4.19−4.36 (m, 1 H). IR (neat, cm^{-1}) ν_{max} 2976, 2881, 1747, 1695, 1392, 1365, 1199, 1157, 1119, 1088, 1033, 999, 974, 922, 888, 858, 772. Identical NMR and IR spectra were observed previously by Kurokawa et al.[71]

6-Oxo-7-oxa-1-azaspiro[4.4]nonane-1-carboxylic Acid *tert*-Butyl Ester (3). To the compound, pyrrolidine-1,2-dicarboxylic acid 1-tert-butyl ester 2-methyl ester **2** (4 g, 17.39 mmol), in dry THF (100 mL) was slowly added lithium diisopropylamide (1.8 M, 18 mL) at −20 °C and the solution stirred for 30 min. The solution was allowed to warm to room temperature and stirred for 1 h. Ethylene oxide gas was slowly bubbled through the solution for 30 min at −20 °C, and the resulting mixture was stirred at room temperature for 12 h. The progress of reaction was monitored by TLC using hexane/EtOAc (7:3). The reaction was quenched by the addition of water and extracted with EtOAc (3 × 30 mL), and the collected organic layer was dried over anhydrous Na_2SO_4 and filtered. The solvent was removed in vacuo, and the residue was purified by passing through the silica gel column using hexane−EtOAc (7:3) as eluent to give the crystalline compound, 6-oxo-7-oxa-1-azaspiro[4.4]nonane-1-carboxylic acid *tert*-butyl ester **3** (3 g, 33.4%): ^{1}H NMR (400 MHz, $CDCl_3$, ppm) δ 1.32 (s, 9H), 1.64−2.14 (m, 5H), 2.53−2.88 (m, 1H), 3.40 (m, 2H), 4.07 (m, 1H), 4.24−4.43 (m, 1H); IR (neat, cm^{-1}) ν_{max} 2975, 2878, 1777, 1690, 1388, 1367, 1205, 1157, 1132, 1107, 1026, 982, 961, 931, 854, 770, 730, 693; EI-MS calcd for $C_{12}H_{19}NO_4$ *m*/*z* 241.13, found 241.07; HRMS calcd for $C_{12}H_{19}NNaO_4^+$ (M + Na^+) *m*/*z* 264.1212, found 264.1201.

7-Oxa-1-azaspiro[4.4]nonan-6-one (4). To compound **3** (1.20 g, 5.0 mmol) in CH_2Cl_2 (10 mL) was slowly added trifluoroacetic acid (TFA) (1 mL) at 0 °C. The mixture was allowed to warm to room temperature and stirred for overnight. The solvent was removed and basified with potassium carbonate and then extracted with EtOAc (3 × 50 mL). The organic layer was collected and dried over anhydrous sodium sulfate and then filtered. The solvent was evaported in vacuo to afford the amine **4** (0.52 g, 76%) and was used without further purification. ^{1}H NMR (400 MHz, $CDCl_3$, ppm) δ 1.88−2.10 (m, 4H), 2.23 (m, 1H), 2.33(m, 1H), 3.05 (m, 1H), 3.28 (m, 1H), 4.21 (q, 1H), 4.39 (m, 1H); IR (neat, cm^{-1}) ν_{max} 3630, 3534, 2983, 1775, 1422, 1379, 1282, 1220, 1191, 1158, 1113, 1023, 959, 793, 693; EI-MS calcd for $C_7H_{11}NO_2$ *m*/*z* 141.1, found 141.0; HRMS calcd for $C_7H_{11}NNaO_2^+$ (M + Na^+) *m*/*z* 164.0687, found 164.0697.

7-Oxa-1-azaspiro[4.4]non-1-en-6-one, 1-Oxide (CPCOMPO). Methyltrioxorhenium(VII) (17.5 mg, 0.07 mmol), EtOH (5 mL), pyridine (28 μL, 0.35 mmol), and 30% H_2O_2 (511 μL, 4.5 mmol) were added sequentially to a 25-mL round bottom flask. A solution of the amino compound **4** (0.5 g, 3.55 mmol) in EtOH (5 mL) was added dropwise at 0 °C. After the mixture was stirred at room temperature for 1 h, 10 mL of water was added. The mixture was extracted with DCM (3 × 30 mL), and the organic phase was dried over $MgSO_4$ concentrated, and purified on silica column using 5% MeOH in DCM (R_f = 0.15) to give white solid product (0.314 g, 57%): ^{1}H NMR (250 MHz, $CDCl_3$, ppm) δ 2.20−2.35 (m, 2H), 2.78 (m, 2H), 3.02 (m, 1H), 3.23 (m, 1H), 4.42 (m, 1H), 4.71 (q, 1H), 6.98 (s, 1H); ^{13}C NMR (250 MHz, $CDCl_3$, ppm) δ 26.2, 30.0, 32.3, 66.6, 78.3, 134.8, 173.8; IR (neat, cm^{-1}) ν 3405, 1769, 1582, 1382, 1226, 1167, 1018; EI-MS calcd for $C_7H_9NO_3$ *m*/*z* 155.06, found 155.0; HRMS calcd for $C_7H_9NNaO_3^+$ (M + Na^+) *m*/*z* 178.0480, found 178.0475.

EPR Measurements. General Methods. EPR measurements were carried out on a Bruker EMX spectrometer equipped with high sensitivity resonator at room temperature. Unless otherwise indicated, the instrument settings used for general spectral acquisition are as follows: microwave power, 20 mW; modulation amplitude, 1.2 G; receiver gain, 3.56 × 10^5; scan time 21 s; time constant, 41 s; sweep width, 80 G. All the spin trapping studies were carried out in a phosphate buffer (PBS) (10 mM) at pH 7.0 containing 100 μM diethylene triamine pentaacetic acid (DTPA). Sample cells used were 50 μL quartz or glass capillary tubes for UV or non-UV irradiation experiments, respectively. The spectrum simulation was carried out using an automatic fitting program.[72]

Spin Trapping. (a) Superoxide Radical Anion. (i) Light Riboflavin. A 50 μL oxygenated PBS solution containing 0.1 mM riboflavin and 50 mM CPCOMPO was irradiated with 150 W light source positioned at 12 cm away from the sample cavity. **(ii) Xanthine−Xanthine Oxidase (X−XO).** A 50 μL PBS solution containing 100 μM DTPA, 0.4 mM xanthine, 0.5 unit/mL xanthine oxidase, and 50 mM CPCOMPO was used. **(iii) KO_2-Generating System.** Superoxide adduct was generated by mixing 25 μL of 100 mM CPCOMPO in PBS and 50 μL of 100 mM KO_2 in DMSO. **(iv) H_2O_2/Pyridine System.** Pseudo-superoxide adduct was generated by mixing 50 mM CPCOMPO with 160 mM H_2O_2 in pyridine. **(b) Hydroxyl Radical.** PBS solution containing 0.2% H_2O_2 and 50 mM CPCOMPO was irradiated for 5 min using a low-pressure mercury vapor lamp at 254 nm wavelength. **(c) Miscellaneous Radicals.** Spin trapping of $SO_3^{\bullet-}$, $CO_2^{\bullet-}$, $CH_3^{\bullet}CHOH$, $GS^{\bullet}$, and $tBuO^{\bullet}$ was carried out in 50 μL PBS solution containing 50 mM CPCOMPO, 0.2% H_2O_2, and 100 mM of the respective radical source $NaHCO_2$, Na_2SO_3, ethanol, GSSG, and $(tBuO)_2$. Each of the mixtures was irradiated with UV for a period of 5 min.

Kinetic Studies (a) Rate Constant of CPCOMPO−O_2H Formation and Decay. Detailed descriptions of the kinetic procedure are given elsewhere,[60,61] and the method used will be only briefly reiterated here. Measurements were made at pH 7 in a 10 mM PBS using a X−XO superoxide generating system. In a typical experiment, a solution contains CPCOMPO (10, 50 or 120 mM), 0.4 mM xanthine, 0.5 unit/mL xanthine oxidase, and 3-carboxy-2,2,5,5-tetramethylpyrrolidin-1-oxyl (3-CP, 1.0 μM) as internal reference. An EPR spectrum of the solution was recorded every 21 s (first recorded at the 42nd s) for ca. 1 h. Noise reduction was accomplished using the singular value decomposition (SVD) procedure. The kinetic curves of the adduct concentration [CPCOMPO−O_2H] as a function of time were obtained after deconvolution of the signal using the pseudo-inverse method.[61] This approach leads to the curves representing only the time evolution of the sole adduct CPCOMPO−O_2H without any contribution from the $HO^{\bullet}$ adduct from a series of EPR spectra composed of mixtures of paramagnetic species with different kinetic formation. These calculations were achieved using a homemade computer program written in FORTRAN, using subroutines given in Numerical Recipes.[73]

Computer modeling of the kinetic curve obtained was achieved using the homemade program Kalidaphnis (formerly Daphnis). The use of this program written in FORTRAN has been described in several papers,[74,75] and it can be obtained upon request from the authors. It allows fitting of experimental curves as signal amplitude or concentration by numerical integration of appropriate rate equations. Application of the standard least-square method yields pertinent kinetic parameters and their respective error values. Using this approach, the curves obtained at the three different initial concentrations of CPCMPO (10, 50, and 120 mM) were considered

(70) Dondoni, A.; Perrone, D. *Org. Synth.* **2000**, *77*, 64.
(71) Kurokawa, M.; Shindo, T.; Suzuki, M.; Nakajima, N.; Ishihara, K.; Sugai, T. *Tetrahedron: Asymmetry* **2003**, *14*, 1323.
(72) Rockenbauer, A.; Korecz, L. *Appl. Magn. Reson.* **1996**, *10*, 29.
(73) Press, W. H.; Teukolsky, S. A.; Vetterling, W. T.; Flannery, B. P. *Numerical Recipes in FORTRAN. The Art of Scientific Computing*, 2nd ed.; Cambridge University Press: Cambridge, 1992.
(74) Mathieu, C.; Tuccio, B.; Lauricella, R.; Mercier, A.; Tordo, P. *J. Chem. Soc., Perkin Trans. 2* **1997**, 2501.
(75) Tuccio, B.; Lauricella, R.; Frejaville, C.; Bouteiller, J.-C.; Tordo, P. *J. Chem. Soc., Perkin Trans. 2* **1995**, 295.

together and modeled using the rate equations shown in Scheme 5, which then led to the k_t and k_d values.

(b) Decay Kinetics of Hydroxyl Radical Adducts. In a typical kinetic study, 50 μL of solution containing 50 mM of CPCOMPO or EMPO and 0.33 mM H_2O_2 was UV irradiated for 3 min in the cavity. The lowest field peak decay was monitored as a function of time over a period of 2680 s after the light source was turned off.

Computational Method. Density functional theory (DFT)[76,77] was applied in this study to determine the optimized geometry, vibrational frequencies, and single-point energy of all stationary points.[78−81] The effect of aqueous solvation was also investigated using the polarizable continuum model (PCM).[82−86] All calculations were performed using Gaussian 03[87] at the Ohio Supercomputer Center. Single-point energies were obtained at the B3LYP/6-31+G** level based on the optimized B3LYP/6-31G* geometries, and the B3LYP/6-31+G**//B3LYP/6-31G* wave functions were used for natural population analyses (NPA).[88] These calculations used six Cartesian d functions. Stationary points for CPCOMPO and the CPCOMPO spin adducts have zero imaginary vibrational frequency as derived from a vibrational frequency analysis (B3LYP/6-31G*). A scaling factor of 0.9806 was used for the zero-point vibrational energy (ZPE) corrections for the B3LYP/6-31G* level.[89] Spin contamination for all of the stationary point of the radical structures was negligible, i.e., $\langle S^2 \rangle = 0.75$. Conformational search of the superoxide adduct complexes with explicit water molecules were carried out using SPARTAN at the MMFF level.

Acknowledgment. This work is supported by NIH Grant No. HL081248. A.R. acknowledges support from the Hungarian Scientific Research Fund, OTKA T-469153. The Ohio Supercomputer Center (OSC) is acknowledged for generous computational support of this research. We thank Prof. David Hart of the OSU Chemistry Department for helpful suggestions and Dr. Judith Galluci for the X-ray measurements. J.L.Z. acknowledges support from the NIH grants HL38324, HL63744, and HL65608.

Supporting Information Available: Spectral characterization data; computional data; crystallographic information files (CIF). This material is available free of charge via the Internet at http://pubs.acs.org.

JO702434U

(76) Labanowski, J. K., Andzelm, J. W., Eds. *Density Functional Methods in Chemistry*; Springer-Verlag: New York, 1991.

(77) Parr, R. G.; Yang, W. *Density-functional Theory of Atoms and Molecules*; Clarendon Press: New York, 1989.

(78) Becke, A. D. *Phys. Rev. A* **1988**, *38*, 3098.

(79) Lee, C.; Yang, W.; Parr, R. G. *Phys. Rev. B* **1988**, *37*, 785.

(80) Becke, A. D. *J. Chem. Phys.* **1993**, *98*, 1372.

(81) Hehre, W. J. R. L.; Schleyer, P. V.; Pople, J. A. *Ab Initio Molecular Orbital Theory*; John Wiley & Sons: New York, 1986.

(82) Barone, V.; Cossi, M.; Tomasi, J. *J. Chem. Phys.* **1997**, *107*, 3210.

(83) Barone, V.; Cossi, M.; Tomasi, J. *J. Comput. Chem.* **1998**, *19*, 404.

(84) Cossi, M.; Barone, V.; Cammi, R.; Tomasi, J. *Chem. Phys. Lett.* **1996**, *255*, 327.

(85) Tomasi, J.; Mennucci, B.; Cammi, R. *Chem. Rev.* **2005**, *105*, 2999.

(86) Tomasi, J.; Persico, M. *Chem. Rev.* **1994**, *94*, 2027.

(87) Frisch, M. J. T. G. W.; Schlegel, H. B.; Scuseria, G. E.; Robb, M. A.; Cheeseman, J. R.; Montgomery, J. A., Jr.; Vreven, T.; Kudin, K. N.; Burant, J. C.; Millam, J. M.; Iyengar, S. S.; Tomasi, J.; Barone, V.; Mennucci, B.; Cossi, M.; Scalmani, G.; Rega, N.; Petersson, G. A.; Nakatsuji, H.; Hada, M.; Ehara, M.; Toyota, K.; Fukuda, R.; Hasegawa, J.; Ishida, M.; Nakajima, T.; Honda, Y.; Kitao, O.; Nakai, H.; Klene, M.; Li, X.; Knox, J. E.; Hratchian, H. P.; Cross, J. B.; Bakken, V.; Adamo, C.; Jaramillo, J.; Gomperts, R.; Stratmann, R. E.; Yazyev, O.; Austin, A. J.; Cammi, R.; Pomelli, C.; Ochterski, J. W.; Ayala, P. Y.; Morokuma, K.; Voth, G. A.; Salvador, P.; Dannenberg, J. J.; Zakrzewski, V. G.; Dapprich, S.; Daniels, A. D.; Strain, M. C.; Farkas, O.; Malick, D. K.; Rabuck, A. D.; Raghavachari, K.; Foresman, J. B.; Ortiz, J. V.; Cui, Q.; Baboul, A. G.; Clifford, S.; Cioslowski, J.; Stefanov, B. B.; Liu, G.; Liashenko, A.; Piskorz, P.; Komaromi, I.; Martin, R. L.; Fox, D. J.; Keith, T.; Al-Laham, M. A.; Peng, C. Y.; Nanayakkara, A.; Challacombe, M.; Gill, P. M. W.; Johnson, B.; Chen, W.; Wong, M. W.; Gonzalez, C.; Pople, J. A. Gaussian 03; Gaussian, Inc: Pittsburgh PA, 2003.

(88) Reed, A. E.; Curtiss, L. A.; Weinhold, F. *Chem. Rev.* **1988**, *88*, 899.

(89) Scott, A. P.; Radom, L. *J. Phys. Chem.* **1996**, *100*, 16502.